

# AWPO: Enhancing Tool-Use of Large Language Models through Explicit Integration of Reasoning Rewards

Zihan Lin <sup>\*1,2</sup> Xiaohan Wang <sup>\*2</sup> Hexiong Yang <sup>1</sup> Jiajun Chai <sup>2</sup> Jie Cao <sup>1</sup> Guojun Yin <sup>†2</sup> Wei Lin <sup>2</sup> Ran He <sup>†1</sup>

## Abstract

While reinforcement learning (RL) shows promise in training tool-use large language models (LLMs) using verifiable outcome rewards, existing methods largely overlook the potential of explicit reasoning rewards to bolster reasoning and tool utilization. Furthermore, naively combining reasoning and outcome rewards may yield suboptimal performance or conflict with the primary optimization objective. To address this, we propose advantage-weighted policy optimization (AWPO)—a principled RL framework that effectively integrates explicit reasoning rewards to enhance tool-use capability. AWPO incorporates variance-aware gating and difficulty-aware weighting to adaptively modulate advantages from reasoning signals based on group-relative statistics, alongside a tailored clipping mechanism for stable optimization. Extensive experiments demonstrate that AWPO achieves state-of-the-art performance across standard tool-use benchmarks, significantly outperforming strong baselines and leading closed-source models in challenging multi-turn scenarios. Notably, with exceptional parameter efficiency, our 4B model surpasses Grok-4 by 16.0% in multi-turn accuracy while preserving generalization capability on the out-of-distribution MMLU-Pro benchmark.

## 1. Introduction

Recently, tool-use has emerged as a critical capability for extending the functional scope of large language models (LLMs) beyond their inherent parametric knowledge (Qin et al., 2023). Regarding post-training for tool-use LLMs, supervised fine-tuning (SFT) is often constrained by overfitting to demonstration trajectories (Fu et al., 2025). In contrast, reinforcement learning (RL) promotes exploration,

thereby mitigating these constraints and enhancing generalization (Yue et al., 2025). Consequently, research focus has increasingly shifted toward developing advanced reward systems and RL algorithms specialized for tool-use scenarios (Zeng et al., 2024).

However, most existing RL approaches neglect the explicit utilization of reasoning rewards to enhance the tool-use capabilities of LLMs. Given that externalized reasoning processes significantly improve accuracy and reliability in complex tasks (Wei et al., 2022), we hypothesize that providing explicit feedback on reasoning quality—such as the logical coherence of a plan or the appropriateness of tool selection—can substantially improve performance. A naive strategy involves directly combining reasoning reward signals from judge models with outcome rewards. Yet, such simple integration may interfere with the primary end-to-end optimization objective, leading to suboptimal performance or even degradation. As illustrated in the lower-right panel of Figure 1, simply mixing reasoning rewards (“Mixed Reward GRPO”) yields marginal improvements over standard Group-Relative Policy Optimization (GRPO) and is occasionally outperformed by baselines such as DAPO. Based on theoretical analysis, we attribute this limited improvement to optimization instability caused by conflicts between reasoning and outcome rewards. This raises a critical question: **How can we effectively leverage explicit reasoning rewards to enhance LLM tool-use capabilities without compromising the primary optimization objective?**

To address this, we analyze the underlying causes of reward conflict and redesign the integration mechanism within the RL framework. As illustrated in Figure 1, the proposed advantage-weighted policy optimization (AWPO) adaptively modulates the influence of reasoning rewards based on group-relative statistics. Our approach is grounded in a key insight: **AWPO selectively incorporates reasoning reward signals when the variance induced by the outcome reward is statistically insignificant.** This ensures that reasoning guidance is introduced judiciously, mitigating optimization conflicts while enhancing reasoning fidelity. Our main contributions are summarized as follows:

- 1) We establish a theoretical framework for combining reasoning and outcome rewards within a GRPO framework. By

<sup>1</sup>Institute of Automation, Chinese Academy of Sciences <sup>2</sup>Meituan. Correspondence to: Guojun Yin <yingguojun02@meituan.com>, Ran He <ran.he@ia.ac.cn>.

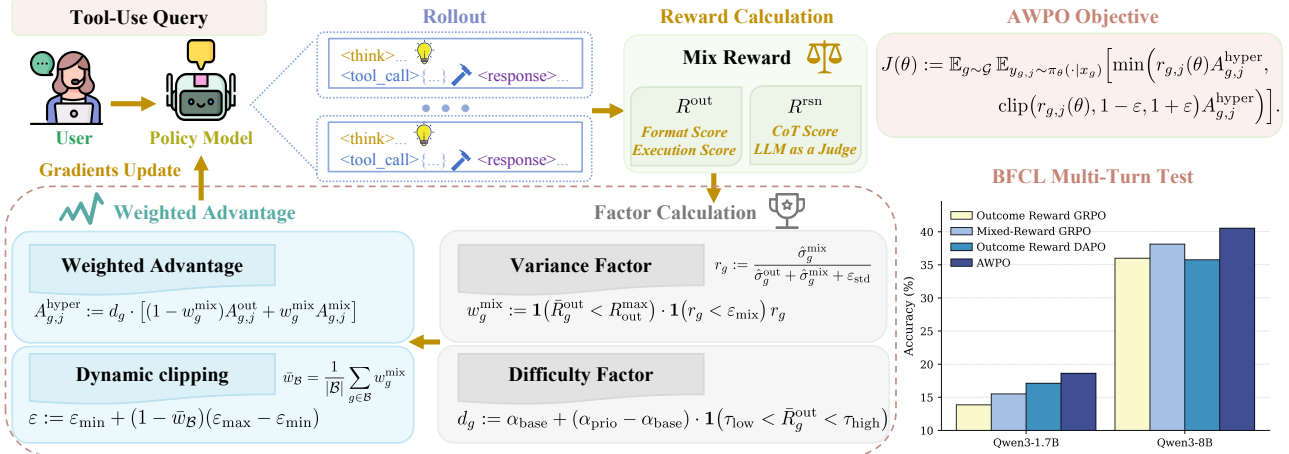


Figure 1: Overview of the AWPO framework. AWPO incorporates variance-aware gating, difficulty-aware weighting, and dynamic clipping mechanisms to effectively achieve reward integration.

deriving an upper bound on the expected policy improvement, we demonstrate that the potential for improvement is governed by a composite signal term, which depends on the alignment of the advantage function with the policy gradient and its variance. This analysis informs the design of the approach, which dynamically adjusts advantage weights to maximize the policy improvement in RL.

2) Building on our theoretical insights, we introduce three novel strategies to realize effective reward integration. First, the variance-aware gating mechanism scales the influence of reasoning rewards based on their discriminative variance relative to outcome rewards within a rollout group. Then, difficulty-aware weighting prioritizes learning from medium-difficulty prompts, where the potential improvement is maximized. To ensure updating stability during backpropagation, we further propose a dynamic clipping strategy that tightens the clipping range.

3) Extensive evaluations on tool-use benchmarks demonstrate that AWPO consistently exceeds strong baselines and the leading closed-source LLMs. In general, AWPO achieves multi-turn accuracy on BFCL by up to 10.50% (a 25.2% relative improvement) and elevates success rates on API-Bank’s hardest Level-3 tasks by 15.27% (a 37.7% relative gain) over the baseline RL method. Notably, AWPO enables a 4B base model to surpass closed-source models on tool-use tasks, specifically outperforming Grok-4 by a remarkable margin 16.00% in multi-turn tool-use accuracy. Additionally, the performance on the out-of-distribution MMLU-Pro benchmark validates the generalization of AWPO by 1.47% improvements compared to base models.

## 2. Related Work

### 2.1. Group Relative Policy Optimization for LLMs

Reinforcement learning has become a pivotal approach for aligning and improving LLMs, evolving from foundational PPO to more efficient GRPO paradigms (Ouyang et al., 2022; Schulman et al., 2017). GRPO replaces value networks with group-relative baselines for advantage estimation, substantially improving training efficiency and scalability (Shao et al., 2024; DeepSeek-AI et al., 2025). Subsequent advances have introduced variants to address specific limitations: DAPO stabilizes long-chain reasoning via decoupled advantage clipping (Yu et al., 2025), while Dr.GRPO removes normalizing terms that inadvertently reward verbose outputs (Liu et al., 2025b). To tackle credit assignment in long-horizon tasks, methods such as GiGPO and IGPO employ structured grouping mechanisms (Feng et al., 2025; Zhao et al., 2025a), and BAPO introduces adaptive clipping for stable off-policy updates (Xi et al., 2025). Despite these algorithmic innovations, existing GRPO-style methods overlooked the strategic integration of explicit reasoning rewards—a missed opportunity given the proven role of reasoning in complex reasoning and tool-calling tasks. Our work bridges this gap by proposing a principled RL framework that dynamically incorporates reasoning signals into advantage estimation, thereby enhancing both reasoning fidelity and tool-use performance.

### 2.2. Post-Training for Tool-Use

Enabling LLMs to reliably interact with external tools through multi-step planning is a core challenge in building agentic systems (Qin et al., 2023; Liu et al., 2025a; Zhang et al., 2024; Chen et al., 2025). On the supervised front, BalanceSFT balances reasoning and function-call tokens

while resampling hard examples to improve fine-tuning efficacy (Hao et al., 2025). In contrast, SwiRL extends this idea by synthesizing multi-step tool-use trajectories for step-wise optimization (Goldie et al., 2025). ToolRL demonstrates that GRPO with decomposed rewards outperforms pure SFT on tool-selection benchmarks (Qian et al., 2025), while ResT introduces entropy-guided gradient updates to refine token-level decisions (Lin et al., 2025b). Although these methods advance tool-use capability, they predominantly rely on final-answer outcome rewards and neglect structured reasoning feedback as an explicit training signal.

### 2.3. LLM-as-a-Judge for Reward Design

Automated evaluation of reasoning quality increasingly relies on LLM-as-a-Judge paradigms, where a dedicated LLM scorer rates candidate responses based on structured rubrics (Gu et al., 2025). Early benchmarks such as MT-Bench and AlpacaEval employed GPT-family judges to produce scalar or pairwise scores that correlate well with human preferences (Bai et al., 2024; Dubois et al., 2024). Crowdsourced platforms like Chatbot Arena further popularized pairwise judging for model ranking (Chiang et al., 2024; Li et al., 2024). Recently, such automated scores have been integrated into RL pipelines to optimize reasoning and code-generation models without direct human annotation (Lee et al.; Lambert et al., 2025). To mitigate potential scorer biases, subsequent studies introduced calibration and reweighting techniques (Li et al., 2025). Building on these insights, we design a specialized LLM-as-a-Judge module to assess the logical coherence, correctness, and tool-call appropriateness of generated reasoning content. This allows us to derive fine-grained reasoning rewards that complement end-answer correctness, forming a dual-reward signal for policy optimization.

## 3. Method

### 3.1. Theoretical Analysis

**Definition 3.1** (Objective Function). The objective  $J(\theta)$  follows the standard PPO formulation, defined as the expected value of the clipped advantage estimated over trajectories sampled from the old policy  $\pi_{\theta_{\text{old}}}$ :

$$J(\theta) = \mathbb{E}_{s,a \sim \pi_{\theta_{\text{old}}}} \left[ \min \left( r_{\theta}(s,a) \hat{A}, \text{clip}(r_{\theta}(s,a), 1 - \varepsilon, 1 + \varepsilon) \hat{A} \right) \right], \quad (1)$$

where  $r_{\theta}(s,a) = \frac{\pi_{\theta}(a|s)}{\pi_{\theta_{\text{old}}}(a|s)}$  is the importance-sampling ratio,  $\hat{A}$  denotes the advantage function, and  $\varepsilon > 0$  is the clipping hyperparameter.

**Lemma 3.2** (Expected improvement upper bound). *To analyze the optimization landscape, we assume the objective*

$J : \mathbb{R}^d \rightarrow \mathbb{R}$  admits a smooth approximation satisfying the  $L$ -smoothness condition (Bottou et al., 2018), i.e., for all  $\theta, \theta^+ \in \mathbb{R}^d$ ,

$$J(\theta^+) \leq J(\theta) + \nabla J(\theta)^\top (\theta^+ - \theta) + \frac{L}{2} \|\theta^+ - \theta\|^2. \quad (2)$$

Consider the update

$$\theta^+ := \theta + \alpha \hat{g}, \quad (3)$$

where  $\alpha > 0$  is the learning rate and  $\hat{g}$  is an unbiased gradient estimator,  $\mathbb{E}[\hat{g}] = \nabla J(\theta)$ . Then the expected improvement is bounded by:

$$\mathbb{E}[J(\theta^+) - J(\theta)] \leq \alpha \|\nabla J(\theta)\|^2 + \frac{\alpha^2 L}{2} \mathbb{E}[\|\hat{g}\|^2]. \quad (4)$$

Proof is deferred to Appendix A.1. Equivalently, using the second-moment-variance decomposition (Hofmann et al., 2015) for an unbiased gradient estimator  $\mathbb{E}[\hat{g}]^2 = \|\nabla J(\theta)\|^2 + \text{Var}(\hat{g})$ , we can write

$$\mathbb{E}[J(\theta^+) - J(\theta)] \leq \alpha \|\nabla J(\theta)\|^2 + \frac{\alpha^2 L}{2} \left( \|\nabla J(\theta)\|^2 + \text{Var}(\hat{g}) \right). \quad (5)$$

**Definition 3.3** (Fisher-Normalized Correlation). Let  $Z(s,a) := \nabla_{\theta} \log \pi_{\theta}(a | s) \in \mathbb{R}^d$  denote the score function, and let

$$F := \mathbb{E}[ZZ^\top] \quad (6)$$

be the Fisher information matrix under the sampling distribution of  $(s,a)$ . Define the whitened score

$$U := F^{-1/2} Z, \quad (7)$$

so that  $\mathbb{E}[UU^\top] = I_d$  and in particular  $\mathbb{E}\|U\|^2 = d$ , where  $d$  is the parameter dimension.

Let  $\tilde{A}(s,a)$  be the effective advantage (implicitly defined by the gradient of the objective), with variance  $V := \mathbb{E}[\tilde{A}^2]$ . The Fisher-normalized correlation between  $\tilde{A}$  and whitened score function  $U$  is defined as

$$\rho(\hat{A}) := \frac{\|\mathbb{E}[U \tilde{A}]\|}{\sqrt{dV}}. \quad (8)$$

Intuitively,  $\rho(\hat{A})$  quantifies the alignment between the advantage signal  $\hat{A}$  and the policy's steepest ascent directions encoded by  $U$  in the Fisher geometry.

**Lemma 3.4** (Upper Bound for the Gradient Norm). *Assume the Fisher information matrix  $F$  is positive definite (Kakade, 2001). The squared norm of the policy gradient is upper-bounded by the Fisher-normalized correlation  $\rho(\hat{A})$  and the advantage variance  $V$ :*

$$\|\nabla J(\theta)\|^2 \leq \lambda_{\max}(F) d \rho(\hat{A})^2 V, \quad (9)$$

where  $\lambda_{\max}(F)$  is the maximum eigenvalue of  $F$ . Proof is deferred to Appendix A.2.

Table 1: Comparison on BFCL benchmark across different models. The column abbreviations stand for: **OA** (Overall), **B** (Base), **MF** (Miss Func), **MP** (Miss Param), **LC** (Long Context), **NL** (Non-Live), and **L** (Live).

Models	Parameter	Multi-Turn					Single-Turn		
		OA	B	MF	MP	LC	OA	NL	L
GPT-5-2025-08-07	/	28.50	33.50	29.50	23.00	28.00	65.59	72.92	58.25
Gemini-2.5-Pro	/	25.00	25.50	26.00	24.50	24.00	74.50	85.04	63.95
Amazon-Nova-Pro-v1.0	/	34.75	42.50	24.50	27.50	44.50	81.78	85.25	78.31
Grok-4-0709	/	36.12	44.00	31.00	26.00	43.50	79.80	85.21	74.39
Moonshotai-Kimi-K2-Inst	1000B	41.25	51.00	43.00	31.00	40.00	80.80	84.02	77.57
DeepSeek-R1-0528	671B	44.50	54.50	41.00	36.50	46.00	78.22	75.73	80.90
Qwen3-235B-A22B	235B	40.12	49.00	41.00	29.50	41.00	82.46	87.90	77.03
ToolACE-2-8B	8B	37.00	47.00	31.00	28.00	42.00	82.54	87.87	77.20
BitAgent-8B	8B	37.75	46.50	37.50	24.00	43.00	81.71	87.33	76.09
watt-tool-8B	8B	37.88	45.50	39.00	24.00	43.00	81.71	87.54	75.87
AWPO	4B	<b>52.12</b>	<b>59.00</b>	<b>59.00</b>	<b>39.00</b>	<b>51.50</b>	<b>84.11</b>	<b>87.90</b>	<b>80.32</b>

**Lemma 3.5** (Variance Bound for the Stochastic Gradient). *Consider the mini-batch gradient estimator  $\hat{g} = \frac{1}{B} \sum_{i=1}^B Z_i \tilde{A}_i$ . Under the standard bounded-score assumption from stochastic approximation and actor-critic theory (Konda & Tsitsiklis, 1999), i.e.,  $\|Z\| \leq G_\infty$  for a constant  $G_\infty > 0$ , the variance of the estimator is bounded by:*

$$\text{Var}(\hat{g}) \leq \frac{G_\infty^2}{B} V. \quad (10)$$

*Proof is deferred to Appendix A.3.*

**Theorem 3.6** (Upper-bound signal-variance decomposition). *Combining Lemma 3.2, Lemma 3.4, and Lemma 3.5, the expected improvement for the update  $\theta^+ = \theta + \alpha \hat{g}$  admits the upper bound*

$$\begin{aligned} & \mathbb{E}[J(\theta^+) - J(\theta)] \quad (11) \\ & \leq \alpha \left(1 + \frac{\alpha L}{2}\right) \|\nabla J(\theta)\|^2 + \frac{\alpha^2 L}{2} \text{Var}(\hat{g}) \\ & \leq \underbrace{\alpha \left(1 + \frac{\alpha L}{2}\right) \lambda_{\max}(F) d \rho(\hat{A})^2 V}_{\text{signal}} + \underbrace{\frac{\alpha^2 L}{2} \frac{G_\infty^2}{B} V}_{\text{noise}}. \end{aligned}$$

where  $\rho(\hat{A})$  is the Fisher-normalized correlation from Definition 3.3. Proof is deferred to Appendix A.4.

This theorem reveals that the improvement upper bound—representing the theoretical optimization capacity—scales with the signal term  $\rho(\hat{A})^2 V$ . In rule-based outcome reward settings, the metric fails to assess the quality of the intermediate reasoning content. As training progresses, output diversity diminishes, causing the advantage variance  $V$  to approach zero. This limitation deprives the model of effective guidance for further refining its reasoning capabilities. By introducing an LLM-as-a-Judge to provide

fine-grained scoring of the reasoning content, AWPO effectively increases  $V$ , thereby expanding the optimization potential for high-quality reasoning.

**Theorem 3.7** (Sufficient condition for expanded optimization potential). *Let  $\hat{A}_A$  and  $\hat{A}_B$  be two advantage estimators with variances  $V_A, V_B$  and Fisher-normalized correlations  $\rho_A, \rho_B$ , respectively. Their improvement upper bounds satisfy Theorem 3.6, and the difference between the two upper bounds is given by*

$$\begin{aligned} U_B - U_A &= \alpha \left(1 + \frac{\alpha L}{2}\right) \lambda_{\max}(F) d (\rho_B^2 V_B - \rho_A^2 V_A) \\ &+ \frac{\alpha^2 L}{2} \frac{G_\infty^2}{B} (V_B - V_A). \end{aligned} \quad (12)$$

*In particular, a sufficient condition for the improvement upper bound associated with  $\hat{A}_B$  to strictly exceed that of  $\hat{A}_A$  is:*

$$\rho_B^2 V_B > \rho_A^2 V_A \quad \text{and} \quad V_B \geq V_A. \quad (13)$$

### 3.2. Advantage Weighted Policy Optimization

Our theoretical analysis in Theorem 3.6 highlights a significant limitation characterized by insufficient advantage variance  $V$ , which constrains the theoretical optimization capacity. Guided by this theorem, AWPO leverages an LLM-as-a-Judge to evaluate the quality of the reasoning content, introducing fine-grained rewards to provide precise supervision for gradient updates. To realize effective reward integration, AWPO employs a suite of mechanisms—including variance-aware gating, difficulty-aware weighting, and dynamic clipping.

**Reward Design.** We compute the outcome reward  $R_j^{\text{out}}$  using a set of deterministic rules (Qian et al., 2025) that

checks whether the model emits the required output structure and whether the predicted tool call matches the ground-truth specification. We decompose the outcome reward of the  $j$ -th sample into a format score and an execution score:

$$R_j^{\text{out}} = S_j^{\text{format}} + S_j^{\text{exec}}. \quad (14)$$

The format score uses exact match:

$$S_{j,\text{format}} = \begin{cases} 1, & \text{if the structure is valid,} \\ 0, & \text{otherwise.} \end{cases} \quad (15)$$

For execution correctness, let  $T$  be the ground-truth tool graph and  $P$  the prediction. We assess tool names via Jaccard similarity,

$$r_{\text{name}} = \frac{|N_T \cap N_P|}{|N_T \cup N_P|} \in [0, 1], \quad (16)$$

where  $N_T, N_P$  are the ground-truth and predicted tool-name sets; parameter names, aggregated over tools,

$$r_{\text{para}} = \sum_{T_i \in T} \frac{|P_T(T_i) \cap P_P(T_i)|}{|P_T(T_i) \cup P_P(T_i)|}, \quad (17)$$

and parameter values via exact match,

$$r_{\text{value}} = \sum_{T_i \in T} \sum_{v \in \mathbf{v}(T_i)} \mathbf{1}[P_T(T_i)[v] = P_P(T_i)[v]]. \quad (18)$$

The execution score is the normalized sum

$$S_{j,\text{exec}} = \frac{r_{\text{name}} + r_{\text{para}} + r_{\text{value}}}{1 + |T| + \sum_{T_i \in T} |\mathbf{v}(T_i)|}. \quad (19)$$

The mixed reward for the  $j$ -th sample is defined as

$$R_j^{\text{mix}} = R_j^{\text{out}} + R_j^{\text{reasoning}}, \quad (20)$$

where  $R_j^{\text{reasoning}} \in [0, 1]$  denotes the reasoning quality score assigned by an LLM-as-a-Judge. Specifically, this score reflects the judge model’s assessment of the coherence, logical soundness, completeness, and factual accuracy of the generated chain-of-thought. The detailed prompting strategy and evaluation protocol for the LLM-as-a-Judge are provided in Appendix B.

**Algorithm Design** For each prompt group  $g \in \{1, \dots, G\}$ , we sample  $K$  responses  $\{y_{g,1}, \dots, y_{g,K}\} \sim \pi_\theta(\cdot | x_g)$ . We first compute the per-group sample means and variances of the outcome reward  $R_{g,j}^{\text{out}}$  and the mixed

reward  $R_{g,j}^{\text{mix}}$  separately:

$$\bar{R}_g^{\text{out}} := \frac{1}{K} \sum_{j=1}^K R_{g,j}^{\text{out}}, \quad \bar{R}_g^{\text{mix}} := \frac{1}{K} \sum_{j=1}^K R_{g,j}^{\text{mix}}, \quad (21)$$

$$\hat{V}_g^{\text{out}} := \frac{1}{K} \sum_{j=1}^K (R_{g,j}^{\text{out}} - \bar{R}_g^{\text{out}})^2, \quad (22)$$

$$\hat{V}_g^{\text{mix}} := \frac{1}{K} \sum_{j=1}^K (R_{g,j}^{\text{mix}} - \bar{R}_g^{\text{mix}})^2. \quad (23)$$

Let  $\hat{\sigma}_g^{\text{out}} := \sqrt{\hat{V}_g^{\text{out}}}$  and  $\hat{\sigma}_g^{\text{mix}} := \sqrt{\hat{V}_g^{\text{mix}}}$  denote the standard deviations. Theorem 3.7 identifies  $\rho(\hat{A})^2 V$  as the dominant term in the upper bound, suggesting that—when well-calibrated—the empirical variance  $V$  reflects a reward signal’s discriminative power. Since the mixed reward may offer more informative variation in rule-saturated groups, we define the variance-aware gating weight as:

$$r_g := \frac{\hat{\sigma}_g^{\text{mix}}}{\hat{\sigma}_g^{\text{out}} + \hat{\sigma}_g^{\text{mix}} + \varepsilon_{\text{std}}}, \quad (24)$$

where  $\varepsilon_{\text{std}} > 0$  is a small numerical constant.

To prevent over-reliance on the mixed signal once the outcome objective saturates, we introduce a saturation gate based on the rule mean, where  $R_{\text{out}}^{\text{max}}$  is the peak group-mean of the outcome reward. We also introduce a tolerance parameter  $\varepsilon_{\text{mix}}$  that caps the variance contributed by the LLM-as-a-Judge scores, preventing judge errors from destabilizing training. In light of the signal–noise decomposition in Theorem 3.6,  $\varepsilon_{\text{mix}}$  bounds the variance  $V$ : modest inflation of  $V$ , capturing variability from the reasoning reward, can enhance the signal term  $\rho(\hat{A})^2 V$ , whereas excessive inflation due to judge errors predominantly enlarges the gradient noise  $\text{Var}(\hat{g})$ . We define:

$$w_g^{\text{mix}} := \mathbf{1}(\bar{R}_g^{\text{out}} < R_{\text{out}}^{\text{max}}) \cdot \mathbf{1}(r_g < \varepsilon_{\text{mix}}) r_g, \quad (25)$$

where  $\varepsilon_{\text{mix}}$  sets an upper bound on the acceptable relative dispersion, ensuring that noisy or redundant mixed signals do not dominate learning.

For the  $j$ -th sample in group  $g$ , we compute normalized advantages for the two views using their respective sample statistics:

$$A_{g,j}^{\text{out}} = \frac{R_{g,j}^{\text{out}} - \bar{R}_g^{\text{out}}}{\hat{\sigma}_g^{\text{out}} + \epsilon}, \quad A_{g,j}^{\text{mix}} = \frac{R_{g,j}^{\text{mix}} - \bar{R}_g^{\text{mix}}}{\hat{\sigma}_g^{\text{mix}} + \epsilon}, \quad (26)$$

where  $\epsilon > 0$  is a numerical stabilization constant.

Building upon this mixing strategy, we further modulate the contribution of each group according to its optimization difficulty. Specifically, to mitigate the undue influence of either near-saturated or consistently low-performing prompt

groups during policy optimization (also observed in (Zhan et al., 2025)), we introduce a difficulty-aware group weighting mechanism that depends solely on the outcome reward statistics. We define the group weight  $d_g$  as:

$$d_g := \alpha_{\text{base}} + (\alpha_{\text{prio}} - \alpha_{\text{base}}) \cdot \mathbf{1}(\tau_{\text{low}} < \bar{R}_g^{\text{out}} < \tau_{\text{high}}), \quad (27)$$

where  $\alpha_{\text{prio}} > \alpha_{\text{base}} > 0$  are scaling factors, and  $\tau_{\text{low}}, \tau_{\text{high}}$  are pre-specified difficulty thresholds that identify the intermediate-difficulty regime.

Combining the adaptive mixing weight (Eq. 25) and the difficulty-aware group weight (Eq. 27), the final weighted advantage is given by:

$$A_{g,j}^{\text{hyper}} := d_g [(1 - w_g^{\text{mix}}) A_{g,j}^{\text{out}} + w_g^{\text{mix}} A_{g,j}^{\text{mix}}]. \quad (28)$$

To ensure optimization stability amid the amplified variance, we implement risk-aware adaptive clipping mechanism. Consistent with our theoretical insight that a signal with higher variance necessitates a tighter trust region to bound the noise risk, we dynamically adjust the clip radius based on the batch-level augmentation intensity.

For a training batch  $\mathcal{B}$ , let  $\bar{w}_{\mathcal{B}} = \frac{1}{|\mathcal{B}|} \sum_{g \in \mathcal{B}} w_g^{\text{mix}}$  denote the average reliance on the fine-grained signal. We define the dynamic clip radius  $\varepsilon$  as:

$$\varepsilon := \varepsilon_{\text{min}} + (1 - \bar{w}_{\mathcal{B}})(\varepsilon_{\text{max}} - \varepsilon_{\text{min}}). \quad (29)$$

With the importance sampling ratio  $r_{g,j}(\theta) := \frac{\pi_{\theta}(y_{g,j}|x_g)}{\pi_{\theta_{\text{old}}}(y_{g,j}|x_g)}$ , the final AWPO objective function is formulated as:

$$J(\theta) := \mathbb{E}_{g \sim \mathcal{G}} \mathbb{E}_{y_{g,j} \sim \pi_{\theta}(\cdot|x_g)} \left[ \min \left( r_{g,j}(\theta) A_{g,j}^{\text{hyper}}, \text{clip}(r_{g,j}(\theta), 1 - \varepsilon, 1 + \varepsilon) A_{g,j}^{\text{hyper}} \right) \right]. \quad (30)$$

Complete training procedure is summarized in Algorithm 1.

## 4. Experiments

### 4.1. Experiment Setup

**Training Details** We construct a mixed corpus tailored to robust tool learning in RL. ToolACE (Liu et al., 2025a) (2k multi-turn samples) focuses on the decision of whether to invoke a tool or answer directly in multi-step interactions; Hammer (masked) (Lin et al., 2025a) (1k multi-turn samples) randomizes tool and argument identifiers to enforce description-grounded generalization rather than lexical memorization; and XLAM (Zhang et al., 2024) (11k multi-turn samples and 30k single-turn samples) provides compositional tasks that require issuing one or multiple tool calls per turn. Jointly, these datasets supervise tool-invocation

Table 2: Comparison on BFCL benchmark across different methods. Average performance is calculated using the official scripts. Best results are highlighted in **bold**. The column abbreviations stand for: **NL** (Non-Live), **L** (Live) and **MT** (Multi-Turn).

Method	Overall	Single Turn		MT
		NL	L	
<b>Qwen3-1.7B Models</b>				
Base	54.70%	83.27%	72.95%	8.62%
SFT	57.07%	82.90%	74.06%	14.25%
SFT+GRPO	57.19%	85.31%	72.10%	14.88%
ToolRL	56.78%	85.52%	71.35%	15.50%
Dr.GRPO	57.55%	84.06%	73.66%	15.25%
DAPO	57.53%	84.52%	71.92%	17.12%
AWPO	<b>57.61%</b>	85.52%	70.28%	<b>18.62%</b>
<b>Qwen3-8B Models</b>				
Base	66.34%	88.81%	78.54%	33.00%
SFT	61.39%	82.58%	73.70%	28.00%
SFT+GRPO	64.40%	85.90%	75.70%	32.38%
ToolRL	68.22%	88.50%	80.85%	36.00%
Dr.GRPO	68.15%	88.00%	79.25%	38.12%
DAPO	67.41%	88.27%	79.21%	35.75%
AWPO	<b>69.37%</b>	89.73%	79.16%	<b>40.50%</b>
<b>Qwen3-4B-2507 Models</b>				
Base	71.63%	87.98%	79.52%	48.00%
SFT	71.99%	87.31%	80.63%	48.25%
SFT+GRPO	69.74%	89.46%	80.36%	40.38%
ToolRL	70.40%	89.40%	80.63%	41.62%
Dr.GRPO	71.97%	87.62%	80.19%	48.62%
DAPO	71.15%	89.33%	79.16%	46.25%
AWPO	<b>73.20%</b>	87.90%	80.32%	<b>52.12%</b>

timing, robust semantic grounding, and compositional planning (Qian et al., 2025).

To obtain denser and more fine-grained reward signals, we convert multi-turn dialogue trajectories into single-step decision instances. Concretely, a dialogue with  $K$  interaction steps is decomposed into  $K$  sub-instances, each conditioned on the full preceding context as input and supervised with the model’s action at that step as the target. Furthermore, we augment the chain-of-thought component of each sub-instance by calling GLM-4.6 (Team et al., 2025) and GPT-4o (OpenAI et al., 2024) to generate reference rationales, which are subsequently used by an LLM-as-a-Judge module during training. This decomposition strategy, following the SWiRL framework (Goldie et al., 2025), substantially increases supervision density: the model receives process-level feedback at every decision point rather than only on the final outcome. Such step-wise supervision leads to more stable learning of multi-step reasoning and tool use. We use Swift (Zhao et al., 2025b) and Verl (Sheng et al., 2025) to train models.

**Benchmarks** We evaluate the proposed method on two comprehensive tool-calling benchmarks: the Berkeley Function Calling Leaderboard (BFCL) (Patil et al., 2023), which measures performance on both single-turn and multi-turn tool-use tasks, and API-Bank (Li et al., 2023), a three-tiered suite testing tool invocation in multi-turn dialogues. To isolate the algorithmic contribution, we fine-tune several open-source base models under comparable tool configurations and compare them against strong domain-specific baselines.

Although our method is designed for tool-augmented agents, we also require that the resulting models retain strong general-purpose language understanding beyond the tool-calling setting. To this end, we evaluate on MMLU Pro (Wang et al., 2024), an out-of-distribution multiple-choice QA benchmark that does not involve tool calls. This orthogonal evaluation probes the underlying model’s out-of-distribution generalization and robustness in core language and reasoning skills.

**Baselines** We evaluate a suite of post-training strategies spanning supervised and reinforcement-learning regimes. The **Base Model** is an instruction-tuned backbone without task-specific fine-tuning, serving as the zero-shot reference. **SFT** denotes standard supervised fine-tuning on the task training set with a token-level cross-entropy objective. **GRPO (ToolRL)** (Group Relative Policy Optimization) is an RL-only method widely used for tool-use and reasoning models, directly optimizing a verifiable reward with group-normalized sequence-level advantages. **SFT+GRPO** adopts a two-stage pipeline that first performs SFT and then applies GRPO from the SFT checkpoint, allowing us to measure the marginal effect of RL over a strong supervised baseline. **Dr.GRPO** ("GRPO Done Right") (Liu et al., 2025b) removes standard-deviation normalization in the group-relative advantage and instead uses a mean-centered estimator equivalent up to a constant rescaling to an RLOO-style advantage, reducing bias toward low-variance prompts and length-induced distortions while preserving the GRPO update structure. **DAPO** (Decoupled Clip and Dynamic sAmpling Policy Optimization) (Yu et al., 2025) further refines GRPO-style training by decoupling lower and upper clipping ranges to maintain exploration, combining dynamic sampling with a token-level policy-gradient loss, and using overlong reward shaping to stabilize optimization for long chain-of-thought generations. For a broad comparison, we additionally include similarly sized tool-use models ToolACE2-8B (Liu et al., 2025a), BitAgent-8B, watttool-8B, and ToolACE-MT, as well as large-scale general-purpose models represented by GPT-5 and DeepSeek-R1 (DeepSeek-AI et al., 2025) as external baselines.

Table 3: Comparison on API-Bank benchmark across different methods. Best results are highlighted in **bold**. The column abbreviations stand for: **L1** (Level 1 Acc), **L2** (Level 2 Acc) and **L3** (Level 3 Acc).

Method	Overall	L1	L2	L3
<b>Qwen3-1.7B Models</b>				
Base	47.57%	53.38%	28.36%	39.69%
SFT	58.96%	66.92%	52.24%	38.17%
SFT+GRPO	59.46%	65.91%	58.21%	40.46%
ToolRL	63.65%	70.68%	61.19%	41.22%
Dr.GRPO	54.77%	62.66%	38.81%	38.93%
DAPO	63.48%	69.67%	59.7%	46.56%
AWPO	<b>65.16%</b>	71.93%	61.19%	46.56%
<b>Qwen3-8B Models</b>				
Base	63.32%	70.68%	53.73%	45.80%
SFT	60.64%	69.17%	56.72%	36.64%
SFT+GRPO	63.82%	72.18%	52.22%	42.75%
ToolRL	66.50%	75.44%	64.18%	40.46%
Dr.GRPO	62.48%	71.18%	49.25%	42.75%
DAPO	62.98%	71.18%	52.24%	43.51%
AWPO	<b>67.67%</b>	72.68%	61.19%	55.73%
<b>Qwen3-4B-2507 Models</b>				
Base	66.33%	72.68%	64.18%	48.09%
SFT	60.30%	67.92%	59.70%	37.40%
SFT+GRPO	68.51%	74.44%	65.67%	51.91%
ToolRL	65.33%	71.93%	62.69%	46.56%
Dr.GRPO	65.66%	71.68%	61.19%	49.62%
DAPO	67.34%	73.43%	65.67%	49.62%
AWPO	<b>68.51%</b>	73.93%	65.67%	53.44

## 4.2. Main Results

We evaluate AWPO on two function-calling benchmarks (BFCL and API-Bank) and the out-of-distribution language understanding benchmark MMLU Pro, across three Qwen3 backbones (1.7B, 4B-2507, 8B). Compared with a suite of strong post-training baselines, including ToolRL, Dr.GRPO and DAPO, AWPO consistently improves multi-turn and high-difficulty tool-use performance while preserving or slightly improving single-turn and general language understanding.

**Berkeley Function-Calling Leaderboard.** On BFCL (Tables 1 and 2), AWPO yields the strongest multi-turn performance at all three scales, without sacrificing single-turn accuracy. For Qwen3-4B-2507, multi-turn accuracy increases from 41.62% (ToolRL) to 52.12%, a gain of 10.50 points and a relative improvement of 25.2%, while the overall score improves from 70.40% to 73.20% (+2.80 points). The best alternative RL baseline, Dr.GRPO, reaches 48.62% multi-turn and 71.97% overall, still 3.50 and 1.23 points behind AWPO, respectively. At the 8B scale, AWPO improves multi-turn accuracy from 36.00% (ToolRL) and 38.12% (Dr.GRPO) to 40.50% (+4.50 and +2.38 points), with the

Table 4: Comparison on OOD MMLU Pro benchmark. Average performance is calculated using the official scripts.

Models	Overall Accuracy	Math	Physics	Chemistry	Computer Science	Biology
Qwen3-1.7B-Base	48.60%	56.77%	41.88%	43.64%	41.71%	59.00%
Qwen3-1.7B-AWPO	<b>50.07%</b>	57.81%	43.19%	41.34%	46.34 %	61.65 %
Qwen3-8B-Base	72.10%	80.01%	67.90%	68.63%	65.85%	78.10%
Qwen3-8B-AWPO	<b>72.67%</b>	80.46%	68.51%	67.49%	67.80%	79.08%
Qwen3-4B-2507-Base	72.37%	79.79%	70.13%	67.05%	67.07%	77.82%
Qwen3-4B-2507-AWPO	<b>73.43%</b>	78.90%	71.29%	68.64%	68.78 %	79.50 %

overall score increasing from 68.22% to 69.37% (+1.15 points). For Qwen3-1.7B, AWPO raises multi-turn accuracy from 15.50% (ToolRL) and 17.12% (DAPO) to 18.62%, corresponding to relative gains of 20.1% and 8.8% over the strongest baselines, and slightly improves overall accuracy from 57.55% (Dr.GRPO) to 57.61%.

The external leaderboard comparison in Table 1 further highlights the algorithmic efficiency of AWPO. The 4B AWPO model attains 52.12% multi-turn overall accuracy and 84.11% single-turn overall accuracy, surpassing tool-specialized 8B systems such as ToolACE-2-8B (37.00% multi-turn, 82.54% single-turn) and ToolACE-MT-8B (40.25% multi-turn, 78.23% single-turn). This shows that AWPO achieves a better accuracy–efficiency trade-off.

**API-Bank.** On API-Bank (Table 3), AWPO delivers the strongest or tied-strongest performance at all three scales, with the largest margins on Level-3 (L3), which corresponds to the most compositional and multi-step tasks. For Qwen3-8B, AWPO improves overall accuracy from 66.50% (ToolRL) and 62.98% (DAPO) to 67.67% (+1.17 and +4.69 points, respectively). The L3 accuracy jumps from 40.46% (ToolRL) and 43.51% (DAPO) to 55.73%, i.e., gains of 15.27 and 12.22 points, corresponding to a relative improvement of 37.7% over ToolRL. For Qwen3-4B-2507, AWPO matches the best overall score of 68.51% achieved by SFT+GRPO, while increasing L3 accuracy from 51.91% (SFT+GRPO) and 49.62% (DAPO) to 53.44%. For Qwen3-1.7B, AWPO raises overall accuracy from 63.65% (ToolRL) and 63.48% (DAPO) to 65.16% (+1.51 and +1.68 points), while maintaining the best L3 accuracy of 46.56% and improving L2 from 59.70% (DAPO) to 61.19%. In these challenging tasks (L2/ L3), AWPO successfully expands the boundary of optimization capacity by injecting fine-grained reasoning reward.

**MMLU-Pro** To check whether function-calling RL degrades general language understanding, we evaluate on MMLU Pro (Table 4), which does not involve tool use. AWPO preserves or slightly improves OOD performance at all scales: Qwen3-4B-2507 increases from 72.37% to 73.43% (+1.06 points), Qwen3-8B from 72.10% to 72.67% (+0.57 points), and Qwen3-1.7B from 48.60% to 50.07%

(+1.47 points). The results indicate that AWPO does not overfit to tool-calling patterns or collapse core knowledge, even though training explicitly targets tool-augmented behavior.

In conclusion, AWPO demonstrates consistent superiority across all model scales, particularly in complex, long-horizon reasoning tasks where baselines often stagnate. Besides, this gain is achieved without compromising general reasoning performance. These results confirm that our reward integration mechanisms effectively expand the optimization boundary, establishing AWPO as a robust and efficient paradigm for post-training tool agents.

### 4.3. Ablation Study

We conduct an ablation study on BFCL across the three Qwen3 backbones (Table 5) to isolate the contributions of the main design components in AWPO: difficulty-aware weighting, variance-aware gating, and adaptive clipping.

Removing the difficulty-aware weighting consistently harms multi-turn performance. For Qwen3-4B-2507, multi-turn overall accuracy drops from 52.12% to 44.62% (-7.50 points), and overall BFCL accuracy decreases from 73.20% to 70.05% (-3.15 points). At 8B and 1.7B scales, the same ablation reduces multi-turn accuracy from 40.50% to 38.62% (-1.88 points) and from 18.62% to 15.62% (-3.00 points), respectively, with corresponding overall drops of 1.26 and 0.34 points. This behavior matches the intended role of Eq. 27.

The variance-aware gating exhibits a similarly pronounced effect on multi-turn accuracy. At 4B, relying solely on the mixed reward to calculate advantage—removing the first term in Eq. 28—reduces multi-turn accuracy from 52.12% to 48.12% (-4.00 points) and overall accuracy from 73.20% to 71.51% (-1.69 points). At 8B and 1.7B, the same ablation lowers multi-turn accuracy from 40.50% to 38.12% (-2.38 points) and from 18.62% to 15.50% (-3.12 points), respectively. These performance drops indicate that the variance-aware gating scheme integrates reward signals more effectively than a simple mixed reward.

Finally, fixing the clipping bounds instead of using the adap-

Table 5: Ablation study of AWPO components on the BFCL benchmark across three Qwen3 backbones. **Difficulty-aware weighting** corresponds to the difficulty-aware weighting scheme defined in Eq. 27; **w/o Variance-aware gating** (defined in Eq. 28) refers to the baseline that directly employs the mixed reward for advantage estimation; **Dynamic clipping** replaces the adaptive clipping radius in Eq. 29 with a fixed clipping range.

Models	Overall Acc	Multi-Turn					Single-Turn	
		Overall	Base	Miss Function	Miss Parameter	Long Context	Non Live	Live
<b>Qwen3-1.7B Models</b>								
AWPO	<b>57.61</b>	<b>18.62</b>	22.00	21.50	15.00	16.00	86.17	70.28
w/o difficulty-aware weighting	57.27	15.62	21.50	15.50	12.00	13.50	83.60	73.48
w/o variance-aware gating	56.92	15.50	16.50	20.00	17.00	8.50	83.73	72.28
w/o dynamic clipping	57.54	15.87	19.00	15.00	17.50	12.00	83.44	73.92
<b>Qwen3-8B Models</b>								
AWPO	<b>69.37</b>	<b>40.50</b>	49.50	43.50	34.00	35.00	89.73	79.16
w/o difficulty-aware weighting	68.11	38.62	44.50	42.00	33.50	34.50	89.44	78.50
w/o variance-aware gating	68.13	38.12	45.00	41.50	32.50	33.50	88.98	78.99
w/o dynamic clipping	68.83	39.62	49.00	45.00	30.00	34.50	88.81	79.08
<b>Qwen3-4B-2507 Models</b>								
AWPO	<b>73.20</b>	<b>52.12</b>	59.00	59.00	39.00	51.50	87.90	80.32
w/o difficulty-aware weighting	70.05	44.62	50.50	51.50	31.00	45.50	86.69	79.52
w/o variance-aware gating	71.51	48.12	56.00	54.00	33.50	49.00	86.81	80.05
w/o dynamic clipping	70.71	47.25	58.00	53.50	32.00	45.50	85.81	79.48

tive schedule in Eq. 29 also degrades performance, especially at 4B. Multi-turn accuracy declines from 52.12% to 47.25% (-4.87 points) and overall accuracy from 73.20% to 70.71% (-2.49 points). At 8B and 1.7B, the multi-turn drops are more moderate (from 40.50% to 39.62% and from 18.62% to 15.87%), but still consistent. The results indicate that the adaptive clipping scheme plays a complementary role to difficulty-aware weighting and the variance-aware gating by controlling the noise term in the bound while preserving useful signal.

## 5. Conclusion

In this work, we investigated how to more effectively exploit reasoning supervision when post-training tool-use large language models with reinforcement learning. We proposed AWPO, a GRPO-style policy optimization framework that integrates reasoning rewards into tool-use RL in a theoretically grounded and adaptively controlled manner. Our analysis of expected policy improvement under group-relative advantages highlights the joint role of advantage alignment and variance, clarifying when high-variance reasoning signals are helpful or harmful. Guided by this view, AWPO introduces three components: variance-aware reward integration to effectively integrate reasoning and rule-based signals, difficulty-aware weighting to focus on medium-difficulty groups that yield the most significant gradient update gains, and adaptive clipping to tighten the trust region when optimization relies heavily on high-variance signals.

Experiments on BFCL, API-Bank, and MMLU-Pro demon-

strate that AWPO consistently improves tool-use performance without degrading general language ability. On BFCL, AWPO attains state-of-the-art multi-turn accuracy, e.g., raising Qwen3-4B-2507 to 52.12% multi-turn and 73.20% overall accuracy, with a 25.2% relative gain over strong GRPO-style baselines. On API-Bank, AWPO yields the best or tied-best overall accuracy and large gains on the most compositional Level-3 tasks, while maintaining or slightly improving performance on the out-of-distribution MMLU-Pro benchmark. These results indicate that AWPO turns reasoning from a fragile auxiliary signal into a stable, variance-aware driver of policy improvement, providing a robust paradigm for training LLM-based tool agents and a general recipe for integrating fine-grained reasoning feedback into outcome-driven RL for large language models.

## References

Bai, G., Liu, J., Bu, X., He, Y., Liu, J., Zhou, Z., Lin, Z., Su, W., Ge, T., Zheng, B., et al. Mt-bench-101: A fine-grained benchmark for evaluating large language models in multi-turn dialogues. *arXiv preprint arXiv:2402.14762*, 2024.

Bottou, L., Curtis, F. E., and Nocedal, J. Optimization methods for large-scale machine learning. *SIAM review*, 60(2):223–311, 2018.

Chen, H., Hu, Z., Chai, J., Yang, H., He, H., Wang, X., Lin, W., Wang, L., Yin, G., et al. Toolforge: A data synthesis

---

pipeline for multi-hop search without real-world apis. *arXiv preprint arXiv:2512.16149*, 2025.

Chiang, W.-L., Zheng, L., Sheng, Y., Angelopoulos, A. N., Li, T., Li, D., Zhu, B., Zhang, H., Jordan, M., Gonzalez, J. E., et al. Chatbot arena: An open platform for evaluating llms by human preference. In *Forty-first International Conference on Machine Learning*, 2024.

DeepSeek-AI, Guo, D., Yang, D., Zhang, H., Song, J., Zhang, R., Xu, R., Zhu, Q., Ma, S., Wang, P., Bi, X., Zhang, X., Yu, X., Wu, Y., Wu, Z. F., Gou, Z., Shao, Z., Li, Z., Gao, Z., Liu, A., Xue, B., Wang, B., Wu, B., Feng, B., Lu, C., Zhao, C., Deng, C., Zhang, C., Ruan, C., Dai, D., Chen, D., Ji, D., Li, E., Lin, F., Dai, F., Luo, F., Hao, G., Chen, G., Li, G., Zhang, H., Bao, H., Xu, H., Wang, H., Ding, H., Xin, H., Gao, H., Qu, H., Li, H., Guo, J., Li, J., Wang, J., Chen, J., Yuan, J., Qiu, J., Li, J., Cai, J. L., Ni, J., Liang, J., Chen, J., Dong, K., Hu, K., Gao, K., Guan, K., Huang, K., Yu, K., Wang, L., Zhang, L., Zhao, L., Wang, L., Zhang, L., Xu, L., Xia, L., Zhang, M., Zhang, M., Tang, M., Li, M., Wang, M., Li, M., Tian, N., Huang, P., Zhang, P., Wang, Q., Chen, Q., Du, Q., Ge, R., Zhang, R., Pan, R., Wang, R., Chen, R. J., Jin, R. L., Chen, R., Lu, S., Zhou, S., Chen, S., Ye, S., Wang, S., Yu, S., Zhou, S., Pan, S., Li, S. S., Zhou, S., Wu, S., Ye, S., Yun, T., Pei, T., Sun, T., Wang, T., Zeng, W., Zhao, W., Liu, W., Liang, W., Gao, W., Yu, W., Zhang, W., Xiao, W. L., An, W., Liu, X., Wang, X., Chen, X., Nie, X., Cheng, X., Liu, X., Xie, X., Liu, X., Yang, X., Li, X., Su, X., Lin, X., Li, X. Q., Jin, X., Shen, X., Chen, X., Sun, X., Wang, X., Song, X., Zhou, X., Wang, X., Shan, X., Li, Y. K., Wang, Y. Q., Wei, Y. X., Zhang, Y., Xu, Y., Li, Y., Zhao, Y., Sun, Y., Wang, Y., Yu, Y., Zhang, Y., Shi, Y., Xiong, Y., He, Y., Piao, Y., Wang, Y., Tan, Y., Ma, Y., Liu, Y., Guo, Y., Ou, Y., Wang, Y., Gong, Y., Zou, Y., He, Y., Xiong, Y., Luo, Y., You, Y., Liu, Y., Zhou, Y., Zhu, Y. X., Xu, Y., Huang, Y., Li, Y., Zheng, Y., Zhu, Y., Ma, Y., Tang, Y., Zha, Y., Yan, Y., Ren, Z. Z., Ren, Z., Sha, Z., Fu, Z., Xu, Z., Xie, Z., Zhang, Z., Hao, Z., Ma, Z., Yan, Z., Wu, Z., Gu, Z., Zhu, Z., Liu, Z., Li, Z., Xie, Z., Song, Z., Pan, Z., Huang, Z., Xu, Z., Zhang, Z., and Zhang, Z. Deepseek-r1: Incentivizing reasoning capability in llms via reinforcement learning, 2025. URL <https://arxiv.org/abs/2501.12948>.

Dubois, Y., Galambosi, B., Liang, P., and Hashimoto, T. B. Length-controlled alpacaeval: A simple way to debias automatic evaluators. *arXiv preprint arXiv:2404.04475*, 2024.

Feng, L., Xue, Z., Liu, T., and An, B. Group-in-group policy optimization for llm agent training. *arXiv preprint arXiv:2505.10978*, 2025.

Fu, Y., Chen, T., Chai, J., Wang, X., Tu, S., Yin, G., Lin, W., Zhang, Q., Zhu, Y., and Zhao, D. Srft: A single-stage method with supervised and reinforcement fine-tuning for reasoning. *arXiv preprint arXiv:2506.19767*, 2025.

Goldie, A., Mirhoseini, A., Zhou, H., Cai, I., and Manning, C. D. Synthetic data generation & multi-step rl for reasoning & tool use, 2025. URL <https://arxiv.org/abs/2504.04736>.

Gu, J., Jiang, X., Shi, Z., Tan, H., Zhai, X., Xu, C., Li, W., Shen, Y., Ma, S., Liu, H., Wang, S., Zhang, K., Wang, Y., Gao, W., Ni, L., and Guo, J. A survey on llm-as-a-judge, 2025. URL <https://arxiv.org/abs/2411.15594>.

Hao, B., Xu, Z., Wang, M., Wen, Y., Chen, Y., Peng, C., Chen, L., Wang, D., Zhao, X., Gu, J., Zhuang, C., and Zhang, J. Funreason: Enhancing large language models' function calling via self-refinement multiscale loss and automated data refinement, 2025. URL <https://arxiv.org/abs/2505.20192>.

Hofmann, T., Lucchi, A., Lacoste-Julien, S., and McWilliams, B. Variance reduced stochastic gradient descent with neighbors. *Advances in Neural Information Processing Systems*, 28, 2015.

Kakade, S. M. A natural policy gradient. *Advances in neural information processing systems*, 14, 2001.

Konda, V. and Tsitsiklis, J. Actor-critic algorithms. *Advances in neural information processing systems*, 12, 1999.

Lambert, N., Pyatkin, V., Morrison, J., Miranda, L. J. V., Lin, B. Y., Chandu, K., Dziri, N., Kumar, S., Zick, T., Choi, Y., et al. Rewardbench: Evaluating reward models for language modeling. In *Findings of the Association for Computational Linguistics: NAACL 2025*, pp. 1755–1797, 2025.

Langley, P. Crafting papers on machine learning. In Langley, P. (ed.), *Proceedings of the 17th International Conference on Machine Learning (ICML 2000)*, pp. 1207–1216, Stanford, CA, 2000. Morgan Kaufmann.

Lee, H., Phatale, S., Mansoor, H., Lu, K. R., Mesnard, T., Ferret, J., Bishop, C., Hall, E., Carbune, V., and Rastogi, A. Rlaif: Scaling reinforcement learning from human feedback with ai feedback.

Li, M., Zhao, Y., Yu, B., Song, F., Li, H., Yu, H., Li, Z., Huang, F., and Li, Y. Api-bank: A comprehensive benchmark for tool-augmented llms, 2023. URL <https://arxiv.org/abs/2304.08244>.

Li, Q., Dou, S., Shao, K., Chen, C., and Hu, H. Evaluating scoring bias in llm-as-a-judge, 2025. URL <https://arxiv.org/abs/2506.22316>.

---

Li, T., Chiang, W.-L., Frick, E., Dunlap, L., Wu, T., Zhu, B., Gonzalez, J. E., and Stoica, I. From crowdsourced data to high-quality benchmarks: Arena-hard and benchbuilder pipeline. *arXiv preprint arXiv:2406.11939*, 2024.

Lin, Q., Wen, M., Peng, Q., Nie, G., Liao, J., Wang, J., Mo, X., Zhou, J., Cheng, C., Zhao, Y., Wang, J., and Zhang, W. Robust function-calling for on-device language model via function masking. In *The Thirteenth International Conference on Learning Representations*, 2025a. URL <https://openreview.net/forum?id=yVQcr4qjD6>.

Lin, Z., Wang, X., Cao, J., Chai, J., Yin, G., Lin, W., and He, R. Rest: Reshaping token-level policy gradients for tool-use large language models. *arXiv preprint arXiv:2509.21826*, 2025b.

Liu, W., Huang, X., Zeng, X., Hao, X., Yu, S., Li, D., Wang, S., Gan, W., Liu, Z., Yu, Y., Wang, Z., Wang, Y., Ning, W., Hou, Y., Wang, B., Wu, C., Wang, X., Liu, Y., Wang, Y., Tang, D., Tu, D., Shang, L., Jiang, X., Tang, R., Lian, D., Liu, Q., and Chen, E. Toolace: Winning the points of llm function calling, 2025a. URL <https://arxiv.org/abs/2409.00920>.

Liu, Z., Chen, C., Li, W., Qi, P., Pang, T., Du, C., Lee, W. S., and Lin, M. Understanding r1-zero-like training: A critical perspective. *arXiv preprint arXiv:2503.20783*, 2025b.

OpenAI, :, Hurst, A., Lerer, A., Goucher, A. P., Perelman, A., Ramesh, A., Clark, A., Ostrow, A., Welihinda, A., Hayes, A., Radford, A., Mądry, A., Baker-Whitcomb, A., Beutel, A., Borzunov, A., Carney, A., Chow, A., Kirillov, A., Nichol, A., Paino, A., Renzin, A., Passos, A. T., Kirillov, A., Christakis, A., Conneau, A., Kamali, A., Jabri, A., Moyer, A., Tam, A., Crookes, A., Tootoochian, A., Tootoonchian, A., Kumar, A., Vallone, A., Karpathy, A., Braunstein, A., Cann, A., Codispoti, A., Galu, A., Kondrich, A., Tulloch, A., Mishchenko, A., Baek, A., Jiang, A., Pelisse, A., Woodford, A., Gosalia, A., Dhar, A., Pantuliano, A., Nayak, A., Oliver, A., Zoph, B., Ghorbani, B., Leimberger, B., Rossen, B., Sokolowsky, B., Wang, B., Zweig, B., Hoover, B., Samic, B., McGrew, B., Spero, B., Giertler, B., Cheng, B., Lightcap, B., Walkin, B., Quinn, B., Guaraci, B., Hsu, B., Kellogg, B., Eastman, B., Lugas, C., Wainwright, C., Bassin, C., Hudson, C., Chu, C., Nelson, C., Li, C., Shern, C. J., Conger, C., Barette, C., Voss, C., Ding, C., Lu, C., Zhang, C., Beaumont, C., Hallacy, C., Koch, C., Gibson, C., Kim, C., Choi, C., McLeavey, C., Hesse, C., Fischer, C., Winter, C., Czarnecki, C., Jarvis, C., Wei, C., Koumouzelis, C., Sherburn, D., Kappler, D., Levin, D., Levy, D., Carr, D., Farhi, D., Mely, D., Robinson, D., Sasaki, D., Jin, D., Valladares, D., Tsipras, D., Li, D., Nguyen, D. P., Findlay, D., Oiwoh, E., Wong, E., Asdar, E., Proehl, E., Yang, E., Antonow, E., Kramer, E., Peterson, E., Sigler, E., Wallace, E., Brevdo, E., Mays, E., Khorasani, F., Such, F. P., Raso, F., Zhang, F., von Lohmann, F., Sulit, F., Goh, G., Oden, G., Salmon, G., Starace, G., Brockman, G., Salman, H., Bao, H., Hu, H., Wong, H., Wang, H., Schmidt, H., Whitney, H., Jun, H., Kirchner, H., de Oliveira Pinto, H. P., Ren, H., Chang, H., Chung, H. W., Kivlichan, I., O’Connell, I., O’Connell, I., Osband, I., Silber, I., Sohl, I., Okuyucu, I., Lan, I., Kostrikov, I., Sutskever, I., Kanitscheider, I., Gulrajani, I., Coxon, J., Menick, J., Pachocki, J., Aung, J., Betker, J., Crooks, J., Lennon, J., Kiros, J., Leike, J., Park, J., Kwon, J., Phang, J., Teplitz, J., Wei, J., Wolfe, J., Chen, J., Harris, J., Varavva, J., Lee, J. G., Shieh, J., Lin, J., Yu, J., Weng, J., Tang, J., Yu, J., Jang, J., Candela, J. Q., Beutel, J., Landers, J., Parish, J., Heidecke, J., Schulman, J., Lachman, J., McKay, J., Uesato, J., Ward, J., Kim, J. W., Huizinga, J., Sitkin, J., Kraaijeveld, J., Gross, J., Kaplan, J., Snyder, J., Achiam, J., Jiao, J., Lee, J., Zhuang, J., Harriman, J., Fricke, K., Hayashi, K., Singhal, K., Shi, K., Karthik, K., Wood, K., Rimbach, K., Hsu, K., Nguyen, K., Gu-Lemberg, K., Button, K., Liu, K., Howe, K., Muthukumar, K., Luther, K., Ahmad, L., Kai, L., Itow, L., Workman, L., Pathak, L., Chen, L., Jing, L., Guy, L., Fedus, L., Zhou, L., Mamitsuka, L., Weng, L., McCalum, L., Held, L., Ouyang, L., Feuvrier, L., Zhang, L., Kondraciuk, L., Kaiser, L., Hewitt, L., Metz, L., Doshi, L., Aflak, M., Simens, M., Boyd, M., Thompson, M., Dukhan, M., Chen, M., Gray, M., Hudnall, M., Zhang, M., Aljubeh, M., Litwin, M., Zeng, M., Johnson, M., Shetty, M., Gupta, M., Shah, M., Yatbaz, M., Yang, M. J., Zhong, M., Glaese, M., Chen, M., Janner, M., Lampe, M., Petrov, M., Wu, M., Wang, M., Fradin, M., Pokrass, M., Castro, M., de Castro, M. O. T., Pavlov, M., Brundage, M., Wang, M., Khan, M., Murati, M., Bavarian, M., Lin, M., Yesildal, M., Soto, N., Gimelshein, N., Cone, N., Staudacher, N., Summers, N., LaFontaine, N., Chowdhury, N., Ryder, N., Stathas, N., Turley, N., Tezak, N., Felix, N., Kudige, N., Keskar, N., Deutsch, N., Bundick, N., Puckett, N., Nachum, O., Okelola, O., Boiko, O., Murk, O., Jaffe, O., Watkins, O., Godement, O., Campbell-Moore, O., Chao, P., McMillan, P., Belov, P., Su, P., Bak, P., Bakum, P., Deng, P., Dolan, P., Hoeschele, P., Welinder, P., Tillet, P., Pronin, P., Tillet, P., Dhariwal, P., Yuan, Q., Dias, R., Lim, R., Arora, R., Troll, R., Lin, R., Lopes, R. G., Puri, R., Miyara, R., Leike, R., Gaubert, R., Zamani, R., Wang, R., Donnelly, R., Honsby, R., Smith, R., Sahai, R., Ramchandani, R., Huet, R., Carmichael, R., Zellers, R., Chen, R., Chen, R., Nigmatullin, R., Cheu, R., Jain, S., Altman, S., Schoenholz, S., Toizer, S., Miserendino, S., Agarwal, S., Culver, S., Ethersmith, S., Gray, S., Grove, S., Metzger, S., Hermani, S., Jain, S., Zhao, S., Wu, S., Jomoto, S., Wu, S., Shuaiqi, Xia, Phene, S., Papay, S., Narayanan, S., Coffey, S., Lee, S., Hall, S., Balaji, S., Broda, T., Stramer, T., Xu, T., Gogineni, T., Christian-

---

son, T., Sanders, T., Patwardhan, T., Cunningham, T., Degry, T., Dimson, T., Raoux, T., Shadwell, T., Zheng, T., Underwood, T., Markov, T., Sherbakov, T., Rubin, T., Stasi, T., Kaftan, T., Heywood, T., Peterson, T., Walters, T., Eloundou, T., Qi, V., Moeller, V., Monaco, V., Kuo, V., Fomenko, V., Chang, W., Zheng, W., Zhou, W., Manassra, W., Sheu, W., Zaremba, W., Patil, Y., Qian, Y., Kim, Y., Cheng, Y., Zhang, Y., He, Y., Zhang, Y., Jin, Y., Dai, Y., and Malkov, Y. Gpt-4o system card, 2024. URL <https://arxiv.org/abs/2410.21276>.

Ouyang, L., Wu, J., Jiang, X., Almeida, D., Wainwright, C., Mishkin, P., Zhang, C., Agarwal, S., Slama, K., Ray, A., et al. Training language models to follow instructions with human feedback. *Advances in neural information processing systems*, 35:27730–27744, 2022.

Patil, S. G., Zhang, T., Wang, X., and Gonzalez, J. E. Gorilla: Large language model connected with massive apis, 2023. URL <https://arxiv.org/abs/2305.15334>.

Qian, C., Acikgoz, E. C., He, Q., Wang, H., Chen, X., Hakkani-Tür, D., Tur, G., and Ji, H. Toolrl: Reward is all tool learning needs. *arXiv preprint arXiv:2504.13958*, 2025.

Qin, Y., Liang, S., Ye, Y., Zhu, K., Yan, L., Lu, Y., Lin, Y., Cong, X., Tang, X., Qian, B., et al. Toolllm: Facilitating large language models to master 16000+ real-world apis. *arXiv preprint arXiv:2307.16789*, 2023.

Schulman, J., Wolski, F., Dhariwal, P., Radford, A., and Klimov, O. Proximal policy optimization algorithms. *arXiv preprint arXiv:1707.06347*, 2017.

Shao, Z., Wang, P., Zhu, Q., Xu, R., Song, J., Bi, X., Zhang, H., Zhang, M., Li, Y., Wu, Y., et al. Deepseekmath: Pushing the limits of mathematical reasoning in open language models. *arXiv preprint arXiv:2402.03300*, 2024.

Sheng, G., Zhang, C., Ye, Z., Wu, X., Zhang, W., Zhang, R., Peng, Y., Lin, H., and Wu, C. Hybridflow: A flexible and efficient rlhf framework. In *Proceedings of the Twentieth European Conference on Computer Systems, EuroSys '25*, pp. 1279–1297. ACM, March 2025. doi: 10.1145/3689031.3696075. URL <http://dx.doi.org/10.1145/3689031.3696075>.

Team, ., Zeng, A., Lv, X., Zheng, Q., Hou, Z., Chen, B., Xie, C., Wang, C., Yin, D., Zeng, H., Zhang, J., Wang, K., Zhong, L., Liu, M., Lu, R., Cao, S., Zhang, X., Huang, X., Wei, Y., Cheng, Y., An, Y., Niu, Y., Wen, Y., Bai, Y., Du, Z., Wang, Z., Zhu, Z., Zhang, B., Wen, B., Wu, B., Xu, B., Huang, C., Zhao, C., Cai, C., Yu, C., Li, C., Ge, C., Huang, C., Zhang, C., Xu, C., Zhu, C., Li, C., Yin, C., Lin, D., Yang, D., Jiang, D., Ai, D., Zhu, E., Wang, F., Pan, G., Wang, G., Sun, H., Li, H., Li, H., Hu, H., Zhang, H., Peng, H., Tai, H., Zhang, H., Wang, H., Yang, H., Liu, H., Zhao, H., Liu, H., Yan, H., Liu, H., Chen, H., Li, J., Zhao, J., Ren, J., Jiao, J., Zhao, J., Yan, J., Wang, J., Gui, J., Zhao, J., Liu, J., Li, J., Li, J., Lu, J., Wang, J., Yuan, J., Li, J., Du, J., Du, J., Liu, J., Zhi, J., Gao, J., Wang, K., Yang, L., Xu, L., Fan, L., Wu, L., Ding, L., Wang, L., Zhang, M., Li, M., Xu, M., Zhao, M., Zhai, M., Du, P., Dong, Q., Lei, S., Tu, S., Yang, S., Lu, S., Li, S., Li, S., Shuang-Li, Yang, S., Yi, S., Yu, T., Tian, W., Wang, W., Yu, W., Tam, W. L., Liang, W., Liu, W., Wang, X., Jia, X., Gu, X., Ling, X., Wang, X., Fan, X., Pan, X., Zhang, X., Zhang, X., Fu, X., Zhang, X., Xu, Y., Wu, Y., Lu, Y., Wang, Y., Zhou, Y., Pan, Y., Zhang, Y., Wang, Y., Li, Y., Su, Y., Geng, Y., Zhu, Y., Yang, Y., Li, Y., Wu, Y., Li, Y., Liu, Y., Wang, Y., Li, Y., Zhang, Y., Liu, Z., Yang, Z., Zhou, Z., Qiao, Z., Feng, Z., Liu, Z., Zhang, Z., Wang, Z., Yao, Z., Wang, Z., Liu, Z., Chai, Z., Li, Z., Zhao, Z., Chen, W., Zhai, J., Xu, B., Huang, M., Wang, H., Li, J., Dong, Y., and Tang, J. Glm-4.5: Agentic, reasoning, and coding (arc) foundation models, 2025. URL <https://arxiv.org/abs/2508.06471>.

Wang, Y., Ma, X., Zhang, G., Ni, Y., Chandra, A., Guo, S., Ren, W., Arulraj, A., He, X., Jiang, Z., Li, T., Ku, M., Wang, K., Zhuang, A., Fan, R., Yue, X., and Chen, W. Mmlu-pro: A more robust and challenging multi-task language understanding benchmark, 2024. URL <https://arxiv.org/abs/2406.01574>.

Wei, J., Wang, X., Schuurmans, D., Bosma, M., Xia, F., Chi, E., Le, Q. V., Zhou, D., et al. Chain-of-thought prompting elicits reasoning in large language models. *Advances in neural information processing systems*, 35:24824–24837, 2022.

Xi, Z., Guo, X., Nan, Y., Zhou, E., Shen, J., Chen, W., Liu, J., Huang, J., Zhang, Z., Guo, H., et al. Bapo: Stabilizing off-policy reinforcement learning for llms via balanced policy optimization with adaptive clipping. *arXiv preprint arXiv:2510.18927*, 2025.

Yu, Q., Zhang, Z., Zhu, R., Yuan, Y., Zuo, X., Yue, Y., Dai, W., Fan, T., Liu, G., Liu, L., et al. Dapo: An open-source llm reinforcement learning system at scale. *arXiv preprint arXiv:2503.14476*, 2025.

Yue, C., Dong, C., Gao, Y., He, H., Chai, J., Yin, G., and Lin, W. Promoting efficient reasoning with verifiable stepwise reward. *arXiv preprint arXiv:2508.10293*, 2025.

Zeng, A., Liu, M., Lu, R., Wang, B., Liu, X., Dong, Y., and Tang, J. Agenttuning: Enabling generalized agent abilities for llms. In *Findings of the Association for Computational Linguistics: ACL 2024*, pp. 3053–3077, 2024.

---

Zhan, R., Li, Y., Wang, Z., Qu, X., Liu, D., Shao, J., Wong, D. F., and Cheng, Y. Exgrpo: Learning to reason from experience, 2025. URL <https://arxiv.org/abs/2510.02245>.

Zhang, J., Lan, T., Zhu, M., Liu, Z., Hoang, T., Kokane, S., Yao, W., Tan, J., Prabhakar, A., Chen, H., Liu, Z., Feng, Y., Awalgaonkar, T., Murthy, R., Hu, E., Chen, Z., Xu, R., Niebles, J. C., Heinecke, S., Wang, H., Savarese, S., and Xiong, C. xlam: A family of large action models to empower ai agent systems, 2024. URL <https://arxiv.org/abs/2409.03215>.

Zhao, S., Liu, M., Huang, J., Liu, M., Wang, C., Liu, B., Tian, Y., Pang, G., Bell, S., Grover, A., et al. Inpainting-guided policy optimization for diffusion large language models. *arXiv preprint arXiv:2509.10396*, 2025a.

Zhao, Y., Huang, J., Hu, J., Wang, X., Mao, Y., Zhang, D., Zhang, H., Jiang, Z., Wu, Z., Ai, B., Wang, A., Zhou, W., and Chen, Y. Swift:a scalable lightweight infrastructure for fine-tuning, 2025b. URL <https://arxiv.org/abs/2408.05517>.

## A. Proofs

### A.1. Proof of Lemma 3.2

*Proof.* Based on the assumption that the objective  $J$  admits an  $L$ -smooth approximation, for any  $\theta, \theta' \in \mathbb{R}^d$  we have

$$J(\theta') \leq J(\theta) + \nabla J(\theta)^\top (\theta' - \theta) + \frac{L}{2} \|\theta' - \theta\|^2. \quad (31)$$

Apply (31) with the specific choice

$$\theta' = \theta^+ := \theta + \alpha \hat{g},$$

so that  $\theta' - \theta = \alpha \hat{g}$ . This yields

$$J(\theta^+) \leq J(\theta) + \nabla J(\theta)^\top (\alpha \hat{g}) + \frac{L}{2} \|\alpha \hat{g}\|^2 \quad (32)$$

$$= J(\theta) + \alpha \nabla J(\theta)^\top \hat{g} + \frac{\alpha^2 L}{2} \|\hat{g}\|^2. \quad (33)$$

Subtract  $J(\theta)$  from both sides of (33) to obtain

$$J(\theta^+) - J(\theta) \leq \alpha \nabla J(\theta)^\top \hat{g} + \frac{\alpha^2 L}{2} \|\hat{g}\|^2. \quad (34)$$

Now take expectation with respect to the randomness of  $\hat{g}$  (conditioning on  $\theta$ ). Using the unbiasedness assumption

$$\mathbb{E}[\hat{g}] = \nabla J(\theta),$$

we get from (34):

$$\mathbb{E}[J(\theta^+) - J(\theta)] \leq \alpha \nabla J(\theta)^\top \mathbb{E}[\hat{g}] + \frac{\alpha^2 L}{2} \mathbb{E}[\|\hat{g}\|^2] \quad (35)$$

$$= \alpha \nabla J(\theta)^\top \nabla J(\theta) + \frac{\alpha^2 L}{2} \mathbb{E}[\|\hat{g}\|^2] \quad (36)$$

$$= \alpha \|\nabla J(\theta)\|^2 + \frac{\alpha^2 L}{2} \mathbb{E}[\|\hat{g}\|^2], \quad (37)$$

which is exactly the bound stated in (4).

For the equivalent variance form, observe that

$$\mathbb{E}[\|\hat{g}\|^2] = \mathbb{E}[\|\nabla J(\theta) + (\hat{g} - \nabla J(\theta))\|^2]. \quad (38)$$

Expanding the square inside the expectation gives

$$\|\nabla J(\theta) + (\hat{g} - \nabla J(\theta))\|^2 = \|\nabla J(\theta)\|^2 + 2 \nabla J(\theta)^\top (\hat{g} - \nabla J(\theta)) + \|\hat{g} - \nabla J(\theta)\|^2. \quad (39)$$

Taking expectations on both sides of (39) and using  $\mathbb{E}[\hat{g} - \nabla J(\theta)] = 0$  yields

$$\mathbb{E}[\|\hat{g}\|^2] = \|\nabla J(\theta)\|^2 + 2 \nabla J(\theta)^\top \mathbb{E}[\hat{g} - \nabla J(\theta)] + \mathbb{E}[\|\hat{g} - \nabla J(\theta)\|^2] \quad (40)$$

$$= \|\nabla J(\theta)\|^2 + \mathbb{E}[\|\hat{g} - \nabla J(\theta)\|^2]. \quad (41)$$

By definition,

$$\text{Var}(\hat{g}) := \mathbb{E}[\|\hat{g} - \nabla J(\theta)\|^2],$$

so (41) can be written as

$$\mathbb{E}[\|\hat{g}\|^2] = \|\nabla J(\theta)\|^2 + \text{Var}(\hat{g}). \quad (42)$$

Substituting (42) into (37) gives

$$\mathbb{E}[J(\theta^+) - J(\theta)] \leq \alpha \|\nabla J(\theta)\|^2 + \frac{\alpha^2 L}{2} (\|\nabla J(\theta)\|^2 + \text{Var}(\hat{g})), \quad (43)$$

which matches the alternative form stated in the lemma.  $\square$

---

## A.2. Proof of Lemma 3.4

*Proof.* We first express the policy gradient in the Fisher geometry and then relate its norm to the Fisher-normalized correlation.

Recall that the score function and Fisher information matrix are defined as

$$Z := \nabla_\theta \log \pi_\theta(a | s) \in \mathbb{R}^d, \quad F := \mathbb{E}[ZZ^\top],$$

with  $F \succ 0$  by assumption. Let the effective (centered) advantage be  $\tilde{A}$  with variance

$$V := \mathbb{E}[\tilde{A}^2],$$

and assume the policy gradient admits the REINFORCE form

$$\nabla J(\theta) = \mathbb{E}[Z\tilde{A}]. \quad (44)$$

**Step 1: gradient in whitened (Fisher) coordinates.** Define the whitened score

$$U := F^{-1/2}Z.$$

Then, by construction,

$$\mathbb{E}[UU^\top] = F^{-1/2} \mathbb{E}[ZZ^\top] F^{-1/2} = F^{-1/2} F F^{-1/2} = I, \quad (45)$$

$$\mathbb{E}\|U\|^2 = \text{tr}(\mathbb{E}[UU^\top]) = \text{tr}(I) = d. \quad (46)$$

Using  $Z = F^{1/2}U$ , we can rewrite the gradient (44) as

$$\nabla J(\theta) = \mathbb{E}[Z\tilde{A}] = \mathbb{E}[F^{1/2}U\tilde{A}] = F^{1/2}\mathbb{E}[U\tilde{A}]. \quad (47)$$

**Step 2: spectral bound via Fisher.** Taking the squared norm of (47) and using the symmetry of  $F$ ,

$$\|\nabla J(\theta)\|^2 = \|F^{1/2}\mathbb{E}[U\tilde{A}]\|^2 \quad (48)$$

$$= (\mathbb{E}[U\tilde{A}])^\top F (\mathbb{E}[U\tilde{A}]). \quad (49)$$

Since  $F$  is positive definite, for any  $x \in \mathbb{R}^d$  we have

$$x^\top F x \leq \lambda_{\max}(F) \|x\|^2,$$

where  $\lambda_{\max}(F)$  is the largest eigenvalue of  $F$ . Applying this to  $x = \mathbb{E}[U\tilde{A}]$  in (49) yields

$$\|\nabla J(\theta)\|^2 \leq \lambda_{\max}(F) \|\mathbb{E}[U\tilde{A}]\|^2. \quad (50)$$

**Step 3: relating  $\|\mathbb{E}[U\tilde{A}]\|^2$  to  $\rho(\hat{A})$  and  $V$ .** By Definition 3.3, the Fisher-normalized correlation is

$$\rho(\hat{A}) := \frac{\|\mathbb{E}[U\tilde{A}]\|}{\sqrt{dV}}. \quad (51)$$

Using (46) (where  $\mathbb{E}\|U\|^2 = d$ ) and  $V = \mathbb{E}[\tilde{A}^2]$ , we obtain

$$\|\mathbb{E}[U\tilde{A}]\|^2 = \rho(\hat{A})^2 \mathbb{E}\|U\|^2 \mathbb{E}[\tilde{A}^2] = \rho(\hat{A})^2 dV. \quad (52)$$

**Step 4: combining the bounds.** Substituting (52) into (50) gives

$$\|\nabla J(\theta)\|^2 \leq \lambda_{\max}(F) \|\mathbb{E}[U\tilde{A}]\|^2 \quad (53)$$

$$= \lambda_{\max}(F) d \rho(\hat{A})^2 V, \quad (54)$$

which is exactly the claimed inequality (9).  $\square$

---

### A.3. Proof of Lemma 3.5

*Proof.* We view  $\hat{g}$  as a vector-valued random variable and use

$$\text{Var}(\hat{g}) := \mathbb{E}[\|\hat{g} - \mathbb{E}[\hat{g}]\|^2].$$

Let

$$X_i := Z_i \tilde{A}_i \in \mathbb{R}^d, \quad i = 1, \dots, B,$$

so that

$$\hat{g} = \frac{1}{B} \sum_{i=1}^B X_i.$$

We assume  $\{(Z_i, \tilde{A}_i)\}_{i=1}^B$  are i.i.d. samples from the on-policy distribution, hence  $\{X_i\}_{i=1}^B$  are i.i.d. as well.

**Step 1: variance of the mini-batch average.** Denote  $\mu := \mathbb{E}[X_1] = \mathbb{E}[X_i]$  for all  $i$ . Then

$$\hat{g} - \mathbb{E}[\hat{g}] = \hat{g} - \mu = \frac{1}{B} \sum_{i=1}^B (X_i - \mu).$$

Therefore

$$\text{Var}(\hat{g}) = \mathbb{E}[\|\hat{g} - \mathbb{E}[\hat{g}]\|^2] \tag{55}$$

$$= \mathbb{E}\left[\left\|\frac{1}{B} \sum_{i=1}^B (X_i - \mu)\right\|^2\right]. \tag{56}$$

Expand the squared norm:

$$\left\|\frac{1}{B} \sum_{i=1}^B (X_i - \mu)\right\|^2 = \frac{1}{B^2} \left\langle \sum_{i=1}^B (X_i - \mu), \sum_{j=1}^B (X_j - \mu) \right\rangle \tag{57}$$

$$= \frac{1}{B^2} \sum_{i=1}^B \sum_{j=1}^B \langle X_i - \mu, X_j - \mu \rangle. \tag{58}$$

Taking expectation and using linearity,

$$\text{Var}(\hat{g}) = \mathbb{E}\left[\left\|\frac{1}{B} \sum_{i=1}^B (X_i - \mu)\right\|^2\right] \tag{59}$$

$$= \frac{1}{B^2} \sum_{i=1}^B \sum_{j=1}^B \mathbb{E}[\langle X_i - \mu, X_j - \mu \rangle]. \tag{60}$$

For  $i \neq j$ , independence and identical distribution imply

$$\mathbb{E}[X_i - \mu] = 0, \quad \mathbb{E}[X_j - \mu] = 0,$$

and hence

$$\mathbb{E}[\langle X_i - \mu, X_j - \mu \rangle] = \mathbb{E}[X_i - \mu]^\top \mathbb{E}[X_j - \mu] = 0. \tag{61}$$

Thus, in (60), all cross terms with  $i \neq j$  vanish and we get

$$\text{Var}(\hat{g}) = \frac{1}{B^2} \sum_{i=1}^B \mathbb{E}[\|X_i - \mu\|^2] \tag{62}$$

$$= \frac{1}{B^2} B \mathbb{E}[\|X_1 - \mu\|^2] \tag{63}$$

$$= \frac{1}{B} \text{Var}(X_1). \tag{64}$$

**Step 2: bounding  $\text{Var}(X_1)$  by  $\mathbb{E}\|X_1\|^2$ .** By definition,

$$\text{Var}(X_1) = \mathbb{E}[\|X_1 - \mu\|^2] = \mathbb{E}[\|X_1\|^2] - \|\mu\|^2,$$

so in particular

$$\text{Var}(X_1) \leq \mathbb{E}[\|X_1\|^2]. \quad (65)$$

Combining (64) and (65), we obtain

$$\text{Var}(\hat{g}) \leq \frac{1}{B} \mathbb{E}[\|X_1\|^2]. \quad (66)$$

**Step 3: using the bounded-score assumption.** Recall  $X_1 = Z_1 \tilde{A}_1$  with  $Z_1 = \nabla_\theta \log \pi_\theta(a_1 | s_1)$  and the bounded-score assumption

$$\|Z_1\| \leq G_\infty \quad \text{almost surely.}$$

Then

$$\|X_1\|^2 = \|Z_1 \tilde{A}_1\|^2 = \tilde{A}_1^2 \|Z_1\|^2 \leq G_\infty^2 \tilde{A}_1^2. \quad (67)$$

Taking expectation,

$$\mathbb{E}[\|X_1\|^2] \leq G_\infty^2 \mathbb{E}[\tilde{A}_1^2] = G_\infty^2 V, \quad (68)$$

where  $V = \mathbb{E}[\tilde{A}_1^2]$  is the variance of the effective advantage (by definition, the law of  $\tilde{A}_1$  is the same as that of  $\tilde{A}$ ).

**Step 4: combining the bounds.** Substituting (68) into (66) yields

$$\text{Var}(\hat{g}) \leq \frac{1}{B} \mathbb{E}[\|X_1\|^2] \quad (69)$$

$$\leq \frac{1}{B} G_\infty^2 V. \quad (70)$$

That is,

$$\text{Var}(\hat{g}) \leq \frac{G_\infty^2}{B} V,$$

which proves the claimed bound.  $\square$

#### A.4. Proof of Theorem 3.6

*Proof.* We first rewrite the expected improvement in terms of the true gradient norm and the variance of the stochastic estimator, and then upper bound these quantities using Lemmas 3.4 and 3.5.

**Step 1: smoothness-based upper bound.** By Lemma 3.2 (expected improvement upper bound), for the update  $\theta^+ = \theta + \alpha \hat{g}$  we have

$$\mathbb{E}[J(\theta^+) - J(\theta)] \leq \alpha \|\nabla J(\theta)\|^2 + \frac{\alpha^2 L}{2} \mathbb{E}[\|\hat{g}\|^2]. \quad (71)$$

**Step 2: variance decomposition of  $\mathbb{E}\|\hat{g}\|^2$ .** We express the second moment  $\mathbb{E}\|\hat{g}\|^2$  in terms of the gradient norm and the variance of  $\hat{g}$ . Since  $\hat{g}$  is an unbiased estimator of the gradient, we have

$$\mathbb{E}[\hat{g}] = \nabla J(\theta).$$

Write  $\hat{g}$  as

$$\hat{g} = \nabla J(\theta) + (\hat{g} - \nabla J(\theta)). \quad (72)$$

Taking the squared norm and expanding via  $\|a + b\|^2 = \|a\|^2 + 2a^\top b + \|b\|^2$ , we obtain

$$\|\hat{g}\|^2 = \|\nabla J(\theta) + (\hat{g} - \nabla J(\theta))\|^2 \quad (73)$$

$$= \|\nabla J(\theta)\|^2 + 2 \nabla J(\theta)^\top (\hat{g} - \nabla J(\theta)) + \|\hat{g} - \nabla J(\theta)\|^2. \quad (74)$$

Taking expectations on both sides and using  $\mathbb{E}[\hat{g} - \nabla J(\theta)] = 0$ , we get

$$\mathbb{E}[\|\hat{g}\|^2] = \|\nabla J(\theta)\|^2 + 2 \nabla J(\theta)^\top \mathbb{E}[\hat{g} - \nabla J(\theta)] + \mathbb{E}[\|\hat{g} - \nabla J(\theta)\|^2] \quad (75)$$

$$= \|\nabla J(\theta)\|^2 + \mathbb{E}[\|\hat{g} - \nabla J(\theta)\|^2]. \quad (76)$$

By definition of the vector variance,

$$\text{Var}(\hat{g}) := \mathbb{E}[\|\hat{g} - \nabla J(\theta)\|^2],$$

so we have the variance decomposition identity

$$\mathbb{E}[\|\hat{g}\|^2] = \|\nabla J(\theta)\|^2 + \text{Var}(\hat{g}). \quad (77)$$

Substituting (77) into (71) yields

$$\mathbb{E}[J(\theta^+) - J(\theta)] \leq \alpha \|\nabla J(\theta)\|^2 + \frac{\alpha^2 L}{2} (\|\nabla J(\theta)\|^2 + \text{Var}(\hat{g})) \quad (78)$$

$$= \alpha \left(1 + \frac{\alpha L}{2}\right) \|\nabla J(\theta)\|^2 + \frac{\alpha^2 L}{2} \text{Var}(\hat{g}). \quad (79)$$

This proves the first inequality in (11).

**Step 3: Fisher–correlation bound on the gradient norm.** Lemma 3.4 (upper bound for the gradient norm) assumes that the Fisher information matrix  $F = \mathbb{E}[ZZ^\top]$  is positive definite and that the policy gradient admits the REINFORCE form. Under these conditions, Lemma 3.4 yields

$$\|\nabla J(\theta)\|^2 \leq \lambda_{\max}(F) d \rho(\hat{A})^2 V, \quad (80)$$

where  $\lambda_{\max}(F)$  is the largest eigenvalue of  $F$ ,  $d$  is the parameter dimension,  $V = \mathbb{E}[\tilde{A}^2]$  is the variance of the effective advantage, and  $\rho(\hat{A})$  is the Fisher-normalized correlation from Definition 3.3.

**Step 4: variance bound for the stochastic gradient.** Lemma 3.5 (variance bound for the stochastic gradient) assumes the bounded-score condition  $\|Z\| \leq G_\infty$  almost surely and mini-batch size  $B$  for the estimator  $\hat{g} = \frac{1}{B} \sum_{i=1}^B Z_i \hat{A}_i$ . Under these assumptions,

$$\text{Var}(\hat{g}) \leq \frac{G_\infty^2}{B} V. \quad (81)$$

**Step 5: combining the bounds.** Substituting (80) and (81) into (79), we obtain

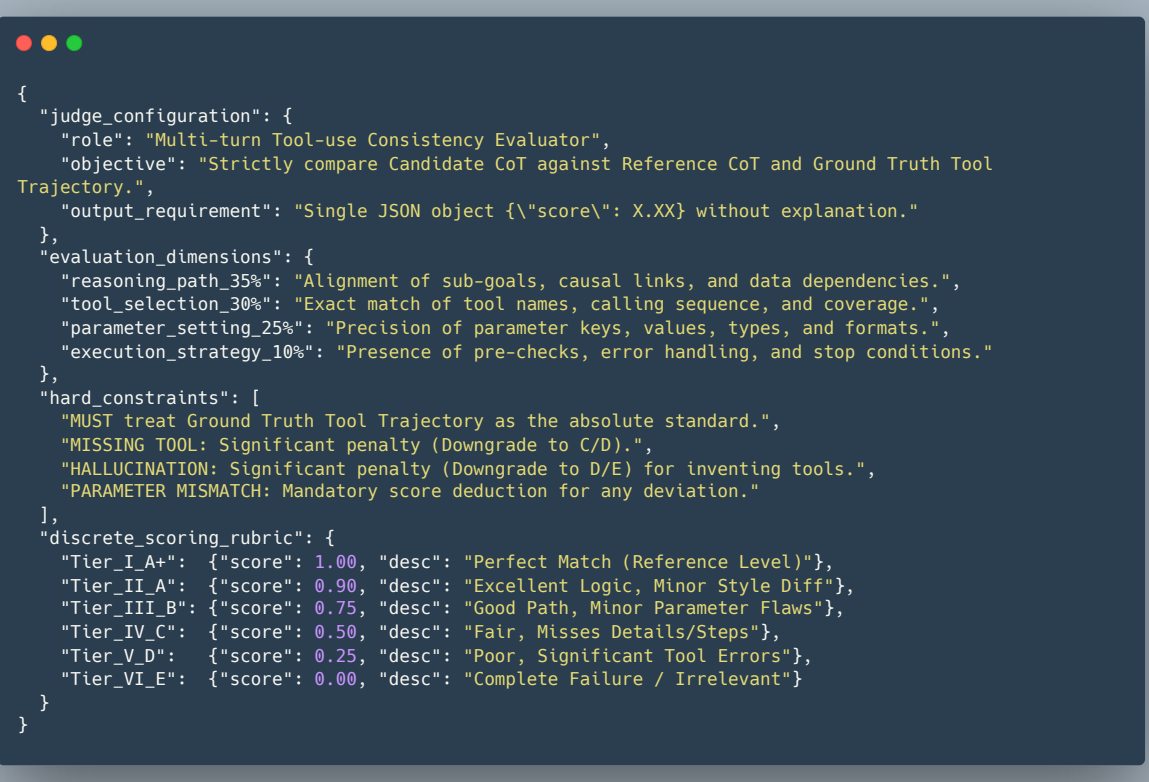
$$\mathbb{E}[J(\theta^+) - J(\theta)] \leq \alpha \left(1 + \frac{\alpha L}{2}\right) \|\nabla J(\theta)\|^2 + \frac{\alpha^2 L}{2} \text{Var}(\hat{g}) \quad (82)$$

$$\leq \alpha \left(1 + \frac{\alpha L}{2}\right) \lambda_{\max}(F) d \rho(\hat{A})^2 V + \frac{\alpha^2 L}{2} \frac{G_\infty^2}{B} V, \quad (83)$$

which is exactly the pair of inequalities stated in (11). The first term corresponds to the **Signal Potential**, proportional to  $\rho(\hat{A})^2 V$ , and the second term represents the **Noise Risk**, proportional to  $V/B$ .  $\square$

## B. LLM as a Judge Design

We employ the Qwen3-235B-A22B model as the LLM-as-a-Judge to evaluate the quality of the generated chain-of-thought outputs in tool-use tasks. To minimize evaluation errors from the LLM-as-a-Judge as much as possible, we constructed reference chains of thought for the training dataset using GPT-4o. During training, when a model receives a low score, the LLM-as-a-Judge is instructed to specifically assess the degree of deviation between the model's generated chain of thought and the corresponding reference chain of thought. Moreover, we also draw inspiration from the approach in (Li et al., 2025) that reduces scoring errors of the LLM-as-a-Judge through carefully crafted prompts, and accordingly designed a tailored set of prompts as shown in Figure 2.



```
{  
  "judge_configuration": {  
    "role": "Multi-turn Tool-use Consistency Evaluator",  
    "objective": "Strictly compare Candidate CoT against Reference CoT and Ground Truth Tool Trajectory.",  
    "output_requirement": "Single JSON object {\\"score\\": X.XX} without explanation."  
  },  
  "evaluation_dimensions": {  
    "reasoning_path_35%": "Alignment of sub-goals, causal links, and data dependencies.",  
    "tool_selection_30%": "Exact match of tool names, calling sequence, and coverage.",  
    "parameter_setting_25%": "Precision of parameter keys, values, types, and formats.",  
    "execution_strategy_10%": "Presence of pre-checks, error handling, and stop conditions."  
  },  
  "hard_constraints": [  
    "MUST treat Ground Truth Tool Trajectory as the absolute standard.",  
    "MISSING TOOL: Significant penalty (Downgrade to C/D).",  
    "HALLUCINATION: Significant penalty (Downgrade to D/E) for inventing tools.",  
    "PARAMETER MISMATCH: Mandatory score deduction for any deviation."  
  ],  
  "discrete_scoring_rubric": {  
    "Tier_I_A+": {"score": 1.00, "desc": "Perfect Match (Reference Level)"},  
    "Tier_II_A": {"score": 0.90, "desc": "Excellent Logic, Minor Style Diff"},  
    "Tier_III_B": {"score": 0.75, "desc": "Good Path, Minor Parameter Flaws"},  
    "Tier_IV_C": {"score": 0.50, "desc": "Fair, Misses Details/Steps"},  
    "Tier_V_D": {"score": 0.25, "desc": "Poor, Significant Tool Errors"},  
    "Tier_VI_E": {"score": 0.00, "desc": "Complete Failure / Irrelevant"}  
  }  
}
```

Figure 2: **Overview of the structured system prompt designed for the Tool-use Consistency Evaluator.** The evaluation protocol is divided into four weighted dimensions: Reasoning Path (35%), Tool Selection (30%), Parameter Setting (25%), and Execution Strategy (10%). To ensure rigorous assessment, the prompt incorporates *hard constraints* based on ground truth tool trajectories and utilizes a *discrete six-tier scoring rubric* (ranging from Tier VI to Tier I) to map qualitative judgments to fixed numerical values (0.00–1.00), thereby reducing variance in the LLM judge's output.

---

## C. Algorithm Details

---

**Algorithm 1** AWPO
 

---

**Input:**  $\{x_g\}_{g=1}^G, \pi_\theta, \theta_{\text{old}}$   
**Hyper:**  $K, \epsilon, \varepsilon_{\text{std}}, \varepsilon_{\text{mix}}, R_{\text{out}}^{\max}, \tau_{\text{low}} < \tau_{\text{high}}, \alpha_{\text{prio}} > \alpha_{\text{base}}, \varepsilon_{\min} \leq \varepsilon_{\max}$

**repeat**

**for**  $g = 1$  **to**  $G$  **do**

Sample  $\{y_{g,j}\}_{j=1}^K \sim \pi_\theta(\cdot | x_g)$ ; obtain  $R_{g,j}^{\text{out}}, R_{g,j}^{\text{mix}}$

$\bar{R}_g^{\text{out}} \leftarrow \frac{1}{K} \sum_{j=1}^K R_{g,j}^{\text{out}}, \bar{R}_g^{\text{mix}} \leftarrow \frac{1}{K} \sum_{j=1}^K R_{g,j}^{\text{mix}}$

$\hat{\sigma}_g^{\text{out}} \leftarrow \sqrt{\frac{1}{K} \sum_{j=1}^K (R_{g,j}^{\text{out}} - \bar{R}_g^{\text{out}})^2}, \hat{\sigma}_g^{\text{mix}} \leftarrow \sqrt{\frac{1}{K} \sum_{j=1}^K (R_{g,j}^{\text{mix}} - \bar{R}_g^{\text{mix}})^2}$

$r_g \leftarrow \frac{\hat{\sigma}_g^{\text{mix}}}{\hat{\sigma}_g^{\text{out}} + \hat{\sigma}_g^{\text{mix}} + \varepsilon_{\text{std}}}$

$w_g^{\text{mix}} \leftarrow \mathbf{1}(\bar{R}_g^{\text{out}} < R_{\text{out}}^{\max}) \cdot \mathbf{1}(r_g < \varepsilon_{\text{mix}}) \cdot r_g$

$d_g \leftarrow \begin{cases} \alpha_{\text{prio}} & \text{if } \tau_{\text{low}} < \bar{R}_g^{\text{out}} < \tau_{\text{high}} \\ \alpha_{\text{base}} & \text{otherwise} \end{cases}$

**end for**

// Compute batch-level clip radius

$\bar{w}_{\mathcal{B}} \leftarrow \frac{1}{G} \sum_{g=1}^G w_g^{\text{mix}}$

$\varepsilon_{\mathcal{B}} \leftarrow \varepsilon_{\min} + (1 - \bar{w}_{\mathcal{B}})(\varepsilon_{\max} - \varepsilon_{\min})$

**for**  $g = 1$  **to**  $G$  **do**

**for**  $j = 1$  **to**  $K$  **do**

$A_{g,j}^{\text{out}} \leftarrow \frac{R_{g,j}^{\text{out}} - \bar{R}_g^{\text{out}}}{\hat{\sigma}_g^{\text{out}} + \epsilon}, A_{g,j}^{\text{mix}} \leftarrow \frac{R_{g,j}^{\text{mix}} - \bar{R}_g^{\text{mix}}}{\hat{\sigma}_g^{\text{mix}} + \epsilon}$

$A_{g,j}^{\text{hyper}} \leftarrow d_g[(1 - w_g^{\text{mix}})A_{g,j}^{\text{out}} + w_g^{\text{mix}}A_{g,j}^{\text{mix}}]$

$r_{g,j}(\theta) \leftarrow \frac{\pi_\theta(y_{g,j} | x_g)}{\pi_{\theta_{\text{old}}}(y_{g,j} | x_g)}$

$\mathcal{L}_{g,j} \leftarrow \min(r_{g,j}(\theta)A_{g,j}^{\text{hyper}}, \text{clip}(r_{g,j}(\theta), 1 - \varepsilon_{\mathcal{B}}, 1 + \varepsilon_{\mathcal{B}})A_{g,j}^{\text{hyper}})$

**end for**

**end for**

$J(\theta) \leftarrow \frac{1}{GK} \sum_{g=1}^G \sum_{j=1}^K \mathcal{L}_{g,j}$

$\theta \leftarrow \theta + \eta \nabla_\theta J(\theta); \theta_{\text{old}} \leftarrow \theta$

**until** converged

---